Distinct Quantal Features of AMPA and NMDA Synaptic Currents in Hippocampal Neurons: Implication of Glutamate Spillover and Receptor Saturation

Yuri V. Pankratov and Oleg A. Krishtal
Bogomoletz Institute of Physiology, Kiev, Ukraine

ABSTRACT Excitatory postsynaptic currents (EPSCs) were studied in the CA1 pyramidal cells of rat hippocampal slices. Components mediated by α-amino-3-hydroxy-5-methylisoxazole-4-proprionic acid (AMPA) and by *N*-methyl-D-aspartate (NMDA) receptors were separated pharmacologically. Quantal parameters of AMPA and NMDA receptor-mediated EPSCs were obtained using both maximal likelihood and autocorrelation techniques. Enhancement of transmitter release with 4-aminopyridine caused a significant increase in quantal size of NMDA EPSC. This was accompanied by a slowing of the EPSC decay. The maximal number of quanta in the NMDA current was unchanged, while the probability of quantal event dramatically enhanced. In contrast, neither the quantal size nor the kinetics of AMPA EPSC was altered by 4-aminopyridine, while the maximal number of quanta increased. These changes in the quantal parameters are consistent with a transition to multivesicular release of the neurotransmitter. Spillover of excessive glutamate on the nonsynaptic areas of dendritic spines causes an increase in the quantal size of NMDA synaptic current. The difference in quantal behavior of AMPA and NMDA EPSCs implies that different mechanisms underlie their quantization: the additive response of nonsaturated AMPA receptors contrasts with the variable involvement of saturated intrasynaptic and nonsaturated extrasynaptic NMDA receptors.

INTRODUCTION

Quantal analysis approaches to transmitter release assume that the release occurs in packets (quanta), and the amplitude of postsynaptic response therefore fluctuates between discrete amplitude levels (Redman, 1990). The quantal parameters of synaptic transmission provide a key for understanding the changes in the synaptic efficacy. In practice, analysis of quantal behavior in central synapses is hampered by factors such as a low signal/noise ratio, the random opening of postsynaptic channels, variability of quantal amplitude, and release probability over release sites. Thus, the quantal behavior of synaptic currents at central synapses has been the subject of much controversy (Larkman et al., 1991; Liao et al., 1992; Kullmann and Nicoll, 1992; Stevens, 1993; Stricker et al., 1996; Liu and Tsien, 1995).

The interpretation of quantal parameters depends on the degree of receptor saturation (Redman, 1990; Voronin, 1993). In the classical case of >presynaptic quantization, the postsynaptic receptors are very far from saturation and a quantum of synaptic current corresponds to the release of a single vesicle, i.e., a quantum of neurotransmitter. When postsynaptic receptors are saturated, a quantum of synaptic current corresponds to the response evoked in a single synaptic bouton (postsynaptic quantization). In this case, the quantal amplitude of postsynaptic response strongly depends on the number of accessible postsynaptic receptors in the vicinity of the release sites.

Submitted November 9, 2002, and accepted for publication July 9, 2003.

Address reprint requests to Yuri V. Pankratov, Institute of Molecular Physiology, University of Sheffield, Alfred Denny Building, Western Bank, Sheffield S10 2TN, UK. E-mail: y.pankratov@sheffield.ac.uk.

0006-3495/03/11/3375/13 $2.00

Spillover of transmitter can increase the number of accessible receptors due to the involvement of extrasynaptic receptors and a possible ''cross talk'' between synapses (Barbour and Hausser, 1997; Asztley et al., 1997). The *N*-methyl-D-aspartate (NMDA) receptors are especially sensitive to these phenomena due to their high affinity to neurotransmitter and slow desensitization. Hence, the impact of glutamate spillover on the quantal features of NMDA and α-amino-3-hydroxy-5-methylisoxazole-4-proprionic acid (AMPA) receptor-mediated components of synaptic transmission may be different (Bergles et al., 1999). Taking into account the different distribution of AMPA and NMDA receptors over synaptic sites in the CA1 hippocampal region (Nusser, 2000), one might expect a large difference in their quantal behavior. Quantal analysis is widely applied for investigation of the potentiation and depression of synaptic transmission (Larkman et al., 1991; Liao et al., 1992; Kullmann and Nicoll, 1992; Stevens, 1993; Larkman et al., 1997). An adequate interpretation of quantal parameters allowing for pre- and/or postsynaptic quantization is very important for the conclusions about the mechanisms of synaptic plasticity. Up to now, the quantal features of the NMDA receptor-mediated component of synaptic transmission have been much less studied than the quantum features of the AMPA component.

Our previous results on the dependence of excitatory postsynaptic current (EPSC) kinetics on stimulus strength (Lozovaya et al., 1999) support the interpretation that glutamate spillover occurred with respect to the NMDA synaptic current. The present paper presents a more detailed investigation of differences in the quantal features of AMPA and NMDA synaptic currents at CA1 synapses of the rat hippocampus, both in control and under conditions of enhanced glutamate release. Two independent techniques,

maximal likelihood and autocorrelation, have been used for reliable evaluation of quantal parameters. The computer simulation of transmitter release and diffusion was used for estimating the effect of spillover and receptor saturation on the amplitude and kinetics of EPSC.

METHODS

Electrophysiology

All experiments were carried out in accordance to European Communities Directives (86/609/EEC). Transverse slices (200–400 μm) of hippocampus were prepared from Wistar rats (17–19 days). The brain was removed rapidly after decapitation and placed into ice-cold artificial cerebrospinal fluid (ACSF-I), containing (mM): NaCl 130, KCl 3, $MgCl_2$ 2.0, NaH_2PO_4 1, $NaHCO_3$ 26, glucose 15, gassed with 95% O_2, 5% CO_2 to obtain a final pH of 7.4. After dissection, the slices were incubated at 32°C for 40 min, then they were kept at room temperature (22–24°C) for 3–6 h before recording (also at room temperature). During incubation and recording, slices were kept in ASCF-II of the following composition (in mM): NaCl 135, KCl 2.7, $CaCl_2$ 2.5, $MgCl_2$ 0.75, NaH_2PO_4 1, $NaHCO_3$ 26, glucose 15, picrotoxin 0.1, gassed with 95% O_2, 5% CO_2 to obtain a final pH of 7.4. Whole-cell voltage clamp recordings were obtained from CA1 neurons using conventional patch-clamp techniques. The patch pipette (1–2.5 MΩ) was filled with the following intracellular solution: CsF 120 mM, Tris-Cl 20 mM, pH 7.3. The series and input resistances were typically 4–12 MΩ and 100–300 MΩ, respectively; they varied by less than 15% in the cells accepted for further analysis. EPSCs were evoked by stimulating the Schaffer collateral/commissural pathway (0.2–0.3 Hz) with a 50 μm Ni/Cr bipolar electrode positioned on the slice surface in the stratum radiatum, at a distance of 50–100 μm from the edge of the stratum pyramidale. The stimulus intensity was reduced until failures appeared. At such stimulus strength the EPSCs still could be reliably evoked and had no sensitivity to the small changes in the stimulus amplitude. 2-Amino-5-phosphonovalerate (D-APV, 20 μM) and 6-cyano-7-nitroquinoxaline-2,3-dione (CNQX, 10 μM) were used for the pharmacological isolation of AMPA and NMDA components of the EPSC. The currents were measured by using an RK400 (BioLogic, Claix, France) amplifier, filtered at 2.0 kHz with a 5-pole Bessel filter, and digitized at 5 kHz.

Data analysis

Currents were analyzed offline. The EPSC peak amplitude was determined using a computer routine based on the fitting of each current trace by a model curve with single exponential rise and decay phases (Fig. 1 *A*). The minimal-square-root procedure was used to determine the amplitude of the model curve, and the time constants and offset were optimized by the gradient method to minimize the mean-square error (Himmelblau, 1972). The time constants of the average current were taken as the initial point for fitting each individual EPSC. The parameters of each model curve were reasonably restricted by the range of 0.5–2 of the initial value. The amplitude of the fitted curve was taken as the EPSC amplitude. Usually the mean-square error of the fit was 5–20% of the EPSC amplitude, depending on baseline noise. Confidence limits for the rise and decay time constants were, respectively, 0.5–1.5 ms, and 2–5 ms for the averaged EPSCs, and 1.5–2.5 ms, and 2–10 ms for individual EPSCs. This method is an outgrowth of the widely used routine where the peak amplitude is determined as the average value in the predefined time window. The amplitude of EPSC calculated according to both methods provides a minimum of mean-square error, but the routine used in the present paper takes into account all the points of current trace, and hence it is less biased.

For analysis of composite EPSCs, two model curves were used for fitting each current trace. The margins for the time constants of the first curve were chosen between the time constants of the fastest and slowest of the pharmacologically isolated AMPA EPSCs, measured in the previous experiments. The margins for the second curve were set using the parameters of the NMDA EPSCs.

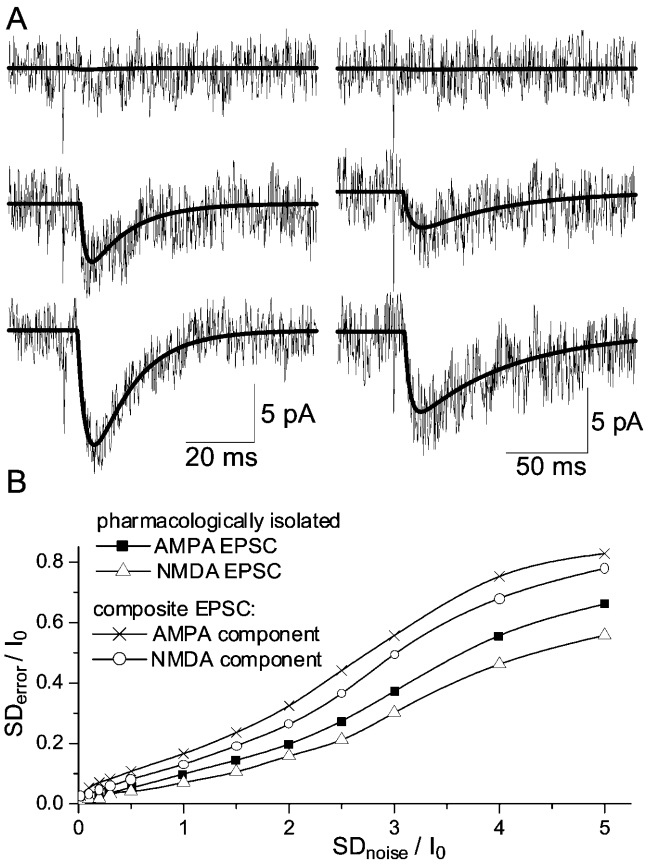

FIGURE 1 Measurement of the amplitude of AMPA and NMDA receptor-mediated synaptic currents. (*A*) Examples of quantal AMPA and NMDA EPSCs. Left: EPSCs recorded in the CA1 pyramidal cell at −75 mV in the presence of 20 μM D-APV. Right: EPSCs recorded at −50 mV in the presence of 10 μM CNQX. The traces were fitted as described in Methods. The thick line represents the model curve with monoexponential rise and decay. The amplitude of this curve was used as the measure of EPSC amplitude. The reliability of this method with respect to noise is illustrated in *B*. *(B)* The dependence of the mean-square error of EPSC amplitude determination (SD_{error}) on the relative noise amplitude was evaluated for pharmacologically isolated AMPA and NMDA EPSCs and the AMPA and NMDA components of composite EPSCs as described in Methods. Note the relative inaccuracy of method is not larger than 20% for noise/signal ratio in the range of 1–2.5.

The reliability of method was confirmed with the aid of the Monte Carlo technique. A set of model EPSCs with random rise and decay times was created. Artificial noise current was generated using a random number generator and added to each parent EPSC. The added noise was simulated as the sum of random values as follows: flat random noise with 2 kHz bandwidth (in accordance to experimental conditions); 50 Hz noise of random amplitude and phase; and a random number of randomly located α-functions with time constant randomly chosen from the ranges of 0.1–1 s and 3–30 ms to simulate the slow and fast fluctuations of holding current. The standard deviation of all the noise components was the same.

In this way a set of 100 EPSCs for testing was obtained for each noise amplitude value. Then the amplitude of each current trace was determined using the method described above. The initial parameters of the fitting curve in each case were chosen randomly and differed from the parameters of the

parent trace by not less than 30%. The error of the method was evaluated as the mean-square deviation of the amplitude of the parent trace:

$$SD_{\text{error}} = \sqrt{\sum_{\text{k}}^{N_{\text{EPSC}}} (I_{\text{fit}}^{\text{k}} - I_0)^2 / N_{\text{EPSC}}}, \quad (1)$$

where SD_{error} is the error of method, I_0 is the amplitude of the parent trace, $I_{\text{fit}}^{\text{k}}$ is the amplitude of the fitting curve for each tested EPSC, and N_{EPSC} is the total number of tested EPSCs.

The error in the EPSC amplitude determination was evaluated for three types of parent traces: pharmacologically isolated AMPA and NMDA currents and the composite EPSC with approximately equal fractions of AMPA and NMDA currents. As one could see from the dependencies of error on the relative noise amplitude (SD_{noise}/I_0) presented in Fig. 1 *B*, the method used provides sufficient accuracy even at twofold noise/signal ratio. Thus, the method used is highly tolerant of noise and enables one to obtain the noise-free amplitude distribution. Usually the set of 700–1500 EPSC amplitudes was obtained and used for statistical analysis in each cell tested. Several subsets of 40 EPSCs were chosen to monitor the slow changes in the mean and coefficient of variation (CV) of current amplitude as well as its kinetics. The data were taken for further analysis only if the mean amplitude, CV, and rise and decay time of EPSC (averaged for each subset) did not undergo significant (>20%) changes in control conditions.

Statistical analysis

The probability density function (PDF) was used for the preliminary assessment. Each value (a_{i}) from a set of EPSC amplitudes was convolved with a normal distribution $G(0, \sigma)$, and the PDF was obtained from:

$$F(a) = \frac{1}{N} \sum_{\text{i}-1}^{\text{N}} G(a_1, \sigma) \quad (2)$$

where N is the sample size. The optimal width of Gaussian kernel σ was chosen as 0.2–0.3 SD_{noise}, where SD_{noise} was the standard deviation of the baseline noise amplitude. Such a value avoids false peaks, and at the same time it is not too large to obscure the quantal features of the PDF (Stricker et al., 1996).

The number of apparent peaks in the PDF and the mean distance between them were taken as preliminary estimates for maximal number of quanta (n) and quantal size (q). The probability of the elementary event (p) could be estimated as m/n, where m is the mean quantal content (evaluated as $1/CV^2$, where CV is variation coefficient). The values of the quantal parameters were adjusted using the binomial model and the likelihood maximization technique (Stricker and Redman, 1994; Stricker et al., 1996). Parameters of the model were fitted directly to the amplitude distribution instead of fitting the amplitude histogram or PDF. Such an approach was helpful to avoid the mistakes related to data sampling. The evaluation of the statistical significance of the quantal model was carried out as described by Stricker and Redman (1994). The quantal binomial model was accepted only if it provided a significantly better fit than the competitive nonquantal model. The nonquantal distribution was calculated as the sum of two Gaussian functions, one of them having a center location set at zero. The center location of the second Gaussian, the widths of both, and their relative fractions were varied to provide a best fit to experimental data. Alternatively, the unimodal distribution calculated as the result of strong smoothing of the experimental PDF was also used as the nonquantal null hypothesis. The binomial distribution was accepted if both nonquantal distributions could be rejected at significance level $\alpha \leq 0.05$.

As an alternative method, we used the autocorrelation (AC)-based method (Stratford et al., 1997) for verifying the quantal features of the amplitude distribution. The autocorrelation–scoring procedure was applied to the PDF for a measured amplitude set, and the AC-function was obtained. The statistical significance of the presence of equally spaced peaks was evaluated with the aid of the Monte Carlo procedure as described in Stratford et al. (1997). The quantal size was determined as the mean period of the AC-function, and the mean quantal content was calculated as the ratio of the mean EPSC amplitude to the quantal size. These values were compared to the data obtained by the likelihood method. A more detailed description of the statistical analysis is given in the Supplementary Material.

Correction for the effect of imperfect voltage-clamp and passive properties of the dendrites

The access resistance and passive electric properties of the cell were evaluated from the current generated by a 5-mV hyperpolarizing step. The measured response was compared with one simulated by cable theory. The simulation was made using the analytical solutions for the current transients (Major et al., 1993) in a passive neuron model with imperfectly clamped soma and two (basal and apical) dendritic cylinders. This model accounts for a somatic shunt resulting from contact with the pipette and uses the following parameters: series resistance (R_{A}), resistance of soma (R_{S}), resistance of somatic shunt (R_{Sh}), resistance of dendritic cable (R_{C}), electrotonic length of the apical and basal dendritic cables (L_{A} and L_{B}), and membrane time constant (τ_{m}). The model uses no preassumptions about cytoplasmic resistivity and specific membrane conductance and capacitance. The values of all parameters were adjusted to provide the best fit of the measured response. The best fit gave realistic values for all the cells tested; the average parameters were as follows: $R_{\text{A}} = 8.2 \pm 4.1$ MΩ, $L_{\text{A}} = 0.99 \pm 0.19$, $\tau_{\text{m}} = 62 \pm 7$ ms, the input resistance of soma (accounting for shunt) $R_{\text{S}}^* = (R_{\text{S}} || R_{\text{Sh}}) = 1190 \pm 630$ MΩ, and cell input resistance $R_{\text{in}} = (R_{\text{S}}^* || R_{\text{C}}) = 149 \pm 51$ MΩ. Next, the postsynaptic currents recorded in the soma of each cell tested were compared with a simulated response to a source current injected in the end of dendritic cable. The source current had mono-exponential rise and decay. Its kinetics and amplitude were adjusted for the best fit of current measured at the soma. This procedure provided an estimation of changes in the amplitude and kinetics of synaptic current as the result of filtering by dendritic tree. To account for possible impact of voltage-clamp conditions on the amplitude and kinetics of EPSC, the same approach was used for monitoring of the input and series resistance and passive properties of dendrites during the recording session.

Simulation of the effect of extrasynaptic glutamate diffusion on the kinetics and amplitude of quantal EPSC

To estimate the influence of glutamate spillover on the kinetics and amplitude of the postsynaptic current, we used a computer simulation based on the simplified description of transmitter diffusion out of the synaptic cleft suggested by Rusakov and Kullmann (1998). The movement of glutamate molecules released from synaptic vesicles was simulated as free two-dimensional diffusion inside of the cylindrical synaptic cleft and as three-dimensional diffusion in the porous medium. The concentration of glutamate calculated for different distance from release site was used as an external parameter for simulation of activity of glutamate receptors. The probability of receptor activation was computed according to generally accepted kinetic schemes for AMPA and NMDA receptors (Lester and Jahr, 1992; Jonas et al., 1993). The time course of activation of AMPA and NMDA receptors after release of a different number of vesicles was calculated, and dependence of the response on the release and uptake of glutamate was analyzed. The detailed description of computer model is given in the Supplementary Material.

To compare the saturation of the receptor at different conditions the Hill equation was used:

$$R^*/R_{\text{max}} = \frac{(G/EC_{50})^{\text{n}}}{1 + (G/EC_{50})^{\text{n}}}, \quad (3)$$

where R_{max} is the maximal limit of response, G is the number of glutamate molecules released, EC_{50} is the dose of glutamate producing half-maximal response, and n is the Hill coefficient.

The EC_{50} value was used in the simulation of quantal behavior of synaptic current. It was assumed that several synaptic sites were activated; the number of vesicles released in each site was determined using the Monte Carlo procedure. The vesicles were assumed to contain a variable number of neurotransmitter molecules. Thus, the content of neurotransmitter released in each synapse was a random value obeying the quantal distribution law. The responses of each individual postsynaptic site were determined as:

$$I = q_i \frac{G}{N}(R^*/R_{max}), \quad (4)$$

where R^* was given by Eq. 3, N is the average number of transmitter molecules in the vesicle, and q_i represents the current generated in the individual postsynaptic site after release of N molecules in the absence of saturation (i.e., when $EC_{50} \rightarrow \infty$). To introduce site-to-site variability, the values of q_i were randomly chosen from Gaussian distribution. All of the individual responses were summed up to give a net synaptic current. In this way, the set of 1000 random EPSC amplitudes was obtained; further analysis was performed using likelihood method.

RESULTS

Quantal features of the pharmacologically isolated NMDA component of EPSC

Pharmacologically isolated NMDA EPSCs were registered and analyzed in the 20 CA1 pyramidal neurons. For 18 cells, clear evidence for quantal behavior was provided by both likelihood and autocorrelation methods (details are in Supplementary Material, Table S1). In these cells the amplitude distributions of the EPSCs were well approximated by a simple binomial law with constant peak width (Fig. 2 *A*). The quantal size was in the range of 2.8 ± 0.8 pA (at holding potential −50 mV). When corrected for the effect of the imperfect voltage clamp and dendritic scaling (see below), the quantal size equals 6.1 ± 1.3 pA, which corresponds to a quantal conductance of 0.1–0.15 nS. Based on the NMDA receptor channel conductance (Spruston et al., 1995) one can calculate that quantal current is generated by opening of some 20–30 NMDA channels. The probability of an elementary event (p) was 0.31 ± 0.15, and the CV was 0.41 ± 0.16.

The most important quantal parameters, quantal size and mean quantal content, were verified using two independent methods. The values of q and m determined by the likelihood method differed by less than 5–10% from the results obtained by the autocorrelation technique. Linear regression analysis (data are shown in Supplementary Material, Fig. S1) revealed a very significant ($P < 0.005$) correlation between the estimates for q and m determined by the two approaches. The combination of two methods is much less sensitive to the artifacts resulting from finite sampling and preassumptions on the distribution law. The likelihood technique does not require the creation of an amplitude histogram or probability density function and fits the parameters of distribution law directly to the experimental set of EPSC amplitudes. The good fit of the theoretical model to the experimental distribution is illustrated by Fig. 2 *A*. In turn, the autocorrelation-based method uses the experimental PDF but does not use any preassumption on the distribution law and is able to reveal the quantal behavior of the experimental amplitude distribution. Hence the methods used allow evaluation of the quantal parameters of the EPSCs with sufficient accuracy and confidence.

The behavior of quantal parameters of NMDA current in conditions of enhanced release of glutamate was studied in 14 cells. 4-aminopyridine (4-AP; 10 μM) caused considerable increase in the mean amplitude and a decrease in the CV of the EPSC. These changes developed in 5–10 min, and the amplitude and CV remained constant thereafter. 4-AP increased both the probability of the quantal event (125 ± 67%, $P < 0.005$, t-test) and the mean quantal content (119 ± 65%, $P < 0.005$). The maximal number of quanta did not change markedly, as illustrated in Fig. 2 *A*. There was no change in the average number of quanta (2 ± 4%, $P > 0.5$). Surprisingly, the enhancement of glutamate release also caused a considerable change in the quantal size. Quantal size increased by more than 10% in 9 of 14 cells tested. The average increase for these cells was 82 ± 42% ($P < 0.01$). This increase was accompanied by noticeable slowing down of EPSC decay (time constant increased by 48 ± 29%, $P < 0.02$). Currents of different amplitudes did not exhibit any difference in their kinetics either in control (Fig. 2 *B*) or after application of 4-AP (Fig. 2 *C*). At the same time, the current in 4-AP was much slower than the control current of the same amplitude (Fig. 2 *D*). The lack of dependence of the EPSC kinetics on its amplitude suggests that the changes in the EPSC kinetics could not be attributed to imperfect voltage clamp of the dendrites. Nevertheless, the passive electric properties of the dendritic cable might affect the amplitude and kinetics of the EPSC because the dendritic attenuation of a synaptic signal is higher for faster synaptic input. Hypothetically, the changes in the quantal size might arise just from the slowing of the synaptic input. The putative impact of 4-AP on whole-cell recording conditions also should be taken into account.

We evaluated the impact of the passive dendritic properties as described in Methods. First, the parameters of the dendritic cable proved to be unaffected by 4-AP. 4-AP did not alter the passive response of the cell to a small depolarizing voltage step. As shown in Fig. 2 *E*, the passive response of the cell could be well approximated by a ''soma and dendritic cylinder'' model with the same set of parameters for control and 4-AP. Second, the values of quantal size and decay time were corrected for filtering by the dendritic cable. These values and model parameters are presented in the Supplementary Material, Table S1. The relative changes in the EPSC decay time plotted versus changes in the quantal size are presented in Fig. 2 *F*. These data demonstrate the correlation between the changes in the quantal amplitude and kinetics of the postsynaptic current under conditions of enhanced neurotransmitter release: the

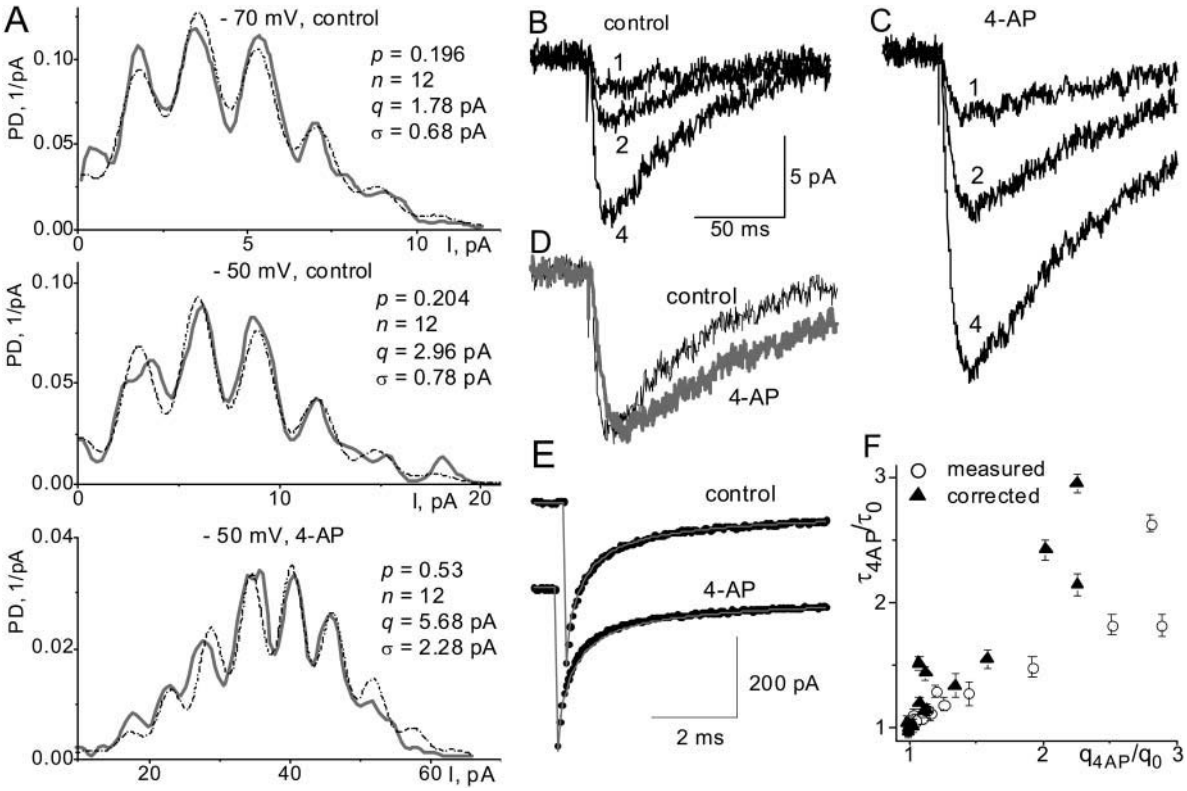

FIGURE 2 Quantal behavior of NMDA EPSC under various experimental conditions. (*A*) The representatives are the probability density function (PDF) for the EPSCs recorded in the CA1 pyramidal neuron (cell 22/01#2, see Table S1) in control and in the presence of 4-AP (10 μM). The quantal parameters calculated by maximal likelihood methods are indicated. The thick gray lines on the left panels represent the PDF for the experimental set of EPSC amplitudes; the dotted lines represent the theoretical PDF of binomial distribution calculated for the values of p,n,q and σ as indicated. Note the close agreement between theoretical and experimental PDFs. The change in the holding voltage altered only the quantal size, whereas the probability and number of quanta remained the same. In turn, 4-AP caused the significant increase in release probability and quantal size but not in number of quanta. (*B–E*) currents recorded from the cell 22/01#2 in control and after bath application of 10 μM 4-AP. (*B*) Average EPSCs corresponding to the different numbers of elementary events in control conditions. Each trace represents the average of 10–20 currents, the amplitude of which falls within the range of $kq \pm \sigma$, where k is the indicated number of quanta, q is quantal size, and σ is variance. (*C*) Average EPSCs corresponding to the different numbers of elementary events in presence of 4-AP. The kinetics of the EPSC does not depend on amplitude in control and under 4-AP as well. (*D*) Superposition of EPSCs corresponding to $k = 4$ quanta in the control and $k = 2$ quanta in 4-AP. These currents have approximately equal amplitudes (11.8 pA in control and 11.4 pA in 4-AP), but their decay times differ considerably (76 ms in control and 123 ms in 4-AP). (*E*) 4-AP does not change the cable properties of dendrites. The points represent the response of the cell to voltage step from -70 to -75 mV before and after application of 4-AP. The difference between data in control and 4-AP could hardly be seen by eye, so the traces were superimposed to the same theoretical curve (*gray solid line*) computed as described in Methods (parameters: access resistance $R_A = 11.3$ MΩ, input resistance $R_{in} = 181$ MΩ, electrotonic cable length $L = 1.1$, membrane time constant $\tau = 59$ ms). (*F*) the ratio of the quantal size of EPSC in 4-AP (q_{4AP}) to the quantal size in control conditions (q_0) is plotted against the ratio of the decay times (τ_{4AP} and τ_0, correspondingly) for 14 cells tested. Two data series are presented: directly measured values (▲) and corresponding values after the correction for imperfect voltage clamp and dendritic filtering (○). A strong correlation exists for both series: the larger the increase in quantal size, the slower the decay of EPSC. These results indicate that the observed changes in the NMDA EPSC kinetics cannot be attributed to the effect of imperfect voltage clamp and dendritic filtering and are related to the changes in the quantal size.

larger the increase in quantal size, the slower the decay of the current. It can be easily seen that the effect of dendritic filtering is not large enough to account for the observed phenomenon. The correlation between changes in the kinetics of synaptic current and quantal amplitude remains strong for the corrected values as well.

Therefore, a purely presynaptic effect of 4-AP is likely to cause the changes in postsynaptic quantal parameters of the NMDA EPSC. The most feasible explanation for the increase in the quantal size is involvement of additional NMDA receptors. Such involvement may result from excessive release of neurotransmitter and its spillover outside the synaptic cleft. Since distant receptors are activated later, increase in synaptic response may also be accompanied by a slowing down of kinetics. The most probable way of enhancement of transmitter release is an increase in the number of vesicles released (transition from mono- to multivesicular release). In this case, enlargement of quantal size may occur only if a single quantum corresponds to the response of the whole postsynaptic site (postsynaptic quantization) rather than the response to each vesicle. This assumption implies saturation of intrasynaptic receptors, which is very likely for NMDA receptors. The extrasynaptic receptors that are exposed to a much lower concentration of

agonist and are not saturated may substantially enhance the quantal synaptic response. Although this hypothesis uses strong assumptions about spillover of glutamate and saturation of receptors, it agrees well with our observations. It is hardly possible to find another explanation for simultaneous increase in quantal size and change in the EPSC kinetics, except increase in the volume of each synaptic vesicle or amount of transmitter contained in the vesicle. In this case the quantal size of AMPA receptor-mediated EPSC would also increased, since AMPA receptors of hippocampal synapses are very likely not saturated (Liu et al., 1999). To decide between two mechanisms of enhancement of synaptic transmission under 4-AP, we therefore studied the changes in quantal parameters of the AMPA component of EPSC.

Quantal features of the pharmacologically isolated AMPA EPSC in the control and in the conditions of the enhanced transmitter release

The pharmacologically isolated AMPA EPSCs were recorded in 10 CA1 pyramidal neurons under the same stimulation conditions as described above for the NMDA EPSC. Statistical analysis carried out in the same way revealed the quantal behavior of the synaptic current in nine cells (details are given in Supplementary Material, Table S2). In these cells the amplitude distribution of the EPSCs also was well approximated by the simple binomial law with constant peak width (Fig. 3 *A*). Quantal size was in the range of 5.7 ± 2.3 pA (holding potential of −70 mV); the ratio of the quantal size to the peak width was in the range of 3.4 ± 0.9.

We did not observe any statistically significant difference in the kinetics of AMPA EPSCs corresponding to their different quantal amplitudes, although the diversity of synaptic currents recorded in the same neuron was quite considerable. The rise and decay time constants varied within the ranges of 2.8 ± 0.5 ms and 25 ± 7 ms, respectively. This variability can be attributed to the considerable impact of the dendritic filtering on the fast AMPA current. The scaling factor for the AMPA EPSC amplitude estimated from the passive electrical properties of the tested neurons was 3.8 ± 1.1. The correction for the dendritic filtering gives the following estimates for the rise and decay time constants: 1.2 ± 0.5 ms and 8.6 ± 2.8 ms. The corrected value for the quantal size is 22.3 ± 6.8 pA, corresponding to a quantal conductance of 0.22–0.42 nS. With the AMPA receptor conductance of 8–10 pS (Jonas et al., 1993; Spruston et al., 1995), this gives 25–50 AMPA channels active per quantal event. Our results are thus in good agreement with the data of Jonas et al. (1993) and Stricker et al. (1996).

The probability of the quantal event for AMPA EPSCs was 0.26 ± 0.11, which is close to the value obtained for the NMDA EPSCs. On the other hand, despite the same stimulation conditions, the maximal number of quanta for AMPA and NMDA currents was different, 10 ± 4 and 14 ± 4, respectively.

Furthermore, the quantal parameters of the AMPA and NMDA EPSCs were altered in different ways under conditions of enhanced neurotransmitter release. 4-AP caused considerable increase in the average amplitude and quantal content of AMPA EPSCs in all of the cells tested ($n = 9$). The pattern of changes was different from NMDA EPSCs, as illustrated in Fig. 3. In contrast to the NMDA current, neither quantal size nor the kinetics of the AMPA current was altered. At the same time, the enhancement of the mean quantal content (m) occurred not only through the increase in the quantal probability (p) but also through the increase in the maximal number of quanta (n). The increase in n was by 84 ± 35% ($P < 0.01$). The average increase in the quantal content of AMPA EPSCs was significantly larger ($P < 0.01$, paired t-test) than the increase in the quantal content of the NMDA EPSCs. Our data demonstrate the distinction between quantal behavior of NMDA and AMPA components of EPSC under conditions of enhanced transmitter release. The changes in quantal size took place only for NMDA current, whereas reliable increase in maximal number of quanta was detected only for AMPA current.

These results argue against the interpretation that vesicle volume is enhanced by 4-AP and strongly support the hypothesis of postsynaptic quantization of NMDA receptors. At the same time, the behavior of the AMPA EPSC may be accounted for by nonsaturation of receptors and presynaptic quantization, for which the quantum represents the response to a single vesicle. To verify the difference in quantal behavior, we analyzed the AMPA and NMDA components of EPSC in one and the same cell, both in the control and in the conditions of the enhanced transmitter release.

Quantal behavior of the simultaneously recorded AMPA and NMDA components of the EPSC

The separation of the AMPA and NMDA components of EPSC was carried out offline, based on the great difference in their kinetics. The technique of EPSC analysis described in the Methods section was modified, and two model curves were used for fitting each current trace (Fig. 4). The margins for the time constants of the first curve were chosen between the time constants of the fastest and slowest pharmacologically isolated AMPA EPSCs, measured in the previous experiments. The margins for the second curve were similarly set using the parameters of the NMDA EPSCs measured by pharmacological isolation.

Hence, the two sets of the amplitudes of AMPA and NMDA components of postsynaptic current were obtained at holding potential −50 mV both before and after applying 4-AP (10 cells). Next, the quantal parameters for each set were calculated in the same way as for the pharmacologically isolated EPSCs using both the likelihood and autocorrela-

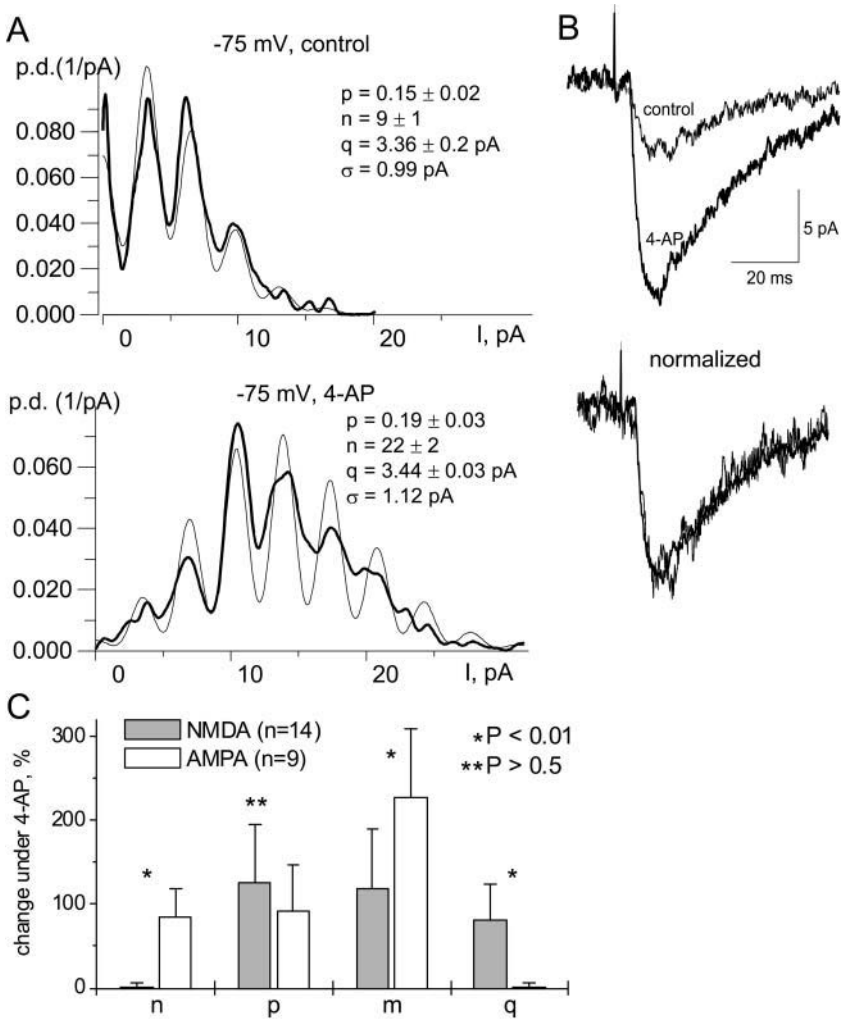

FIGURE 3 Quantal behavior of the AMPA EPSC. (*A*) Results of quantal analysis of pharmacologically isolated AMPA EPSCs. The PDF of the EPSC recorded in cell 14/02#2 (see Table S2) in control conditions and in 4-AP. The quantal parameters calculated by the maximal likelihood method are indicated correspondingly on the left and right panels. The thick lines on the left panels represent PDF for the experimental set of EPSC amplitudes; the thin lines represent PDF calculated for the binomial model for *p*,*n*,*q*, and σ as indicated. (*B*) Average of 10 AMPA EPSCs, recorded in the control and under the action of 4-AP. The superimposed normalized traces (*left*) demonstrate that the kinetics of the current does not undergo considerable changes. (*C*) Comparison of changes in the quantal parameters of AMPA and NMDA currents. Each column represents the relative increase in the maximal number of quanta (*n*), probability of quantal event (*p*), mean quantal content (m) and quantal size (q) caused by 4-AP; asterisks (*) and (**) indicate the statistical significance of difference between AMPA and NMDA EPSC according to the paired *t*-test. Note the different character of changes in the quantal size and maximal number of quanta.

tion methods. To testify the quality of the separation, two additional amplitude sets were obtained in each cell. At the beginning, the amplitude set of AMPA EPSCs was recorded in control conditions at holding potential -80 mV in the presence of 10 μM of D-APV; the D-APV was then washed out and two main datasets were recorded at -50 mV both in control conditions and in 4-AP. Then, CNQX (10 μM) was applied to measure the amplitude set of the NMDA EPSCs. The values of *p* and *n* obtained for the AMPA component at -80 and -50 mV, and the values of *p*, *n*, and *q* for the NMDA component obtained with and without CNQX were compared in pairs (i.e., mathematically isolated versus pharmacologically isolated). In 7 of the 10 cells tested these estimates differed by less than 20% for both AMPA and NMDA components. The data for these cells were used for further analysis.

During recording of the composite EPSCs we found that the AMPA and NMDA components fluctuated in different ways. Frequently the current was decaying down to zero at 40 ms after the peak so it could be almost entirely attributed to AMPA receptors, but sometimes one could see that the current remained considerable even 100 ms after peak, indicating a large contribution of NMDA receptors (Fig. 4). Of course, the kinetics of EPSCs generated at different synaptic sites can be slowed to a different extent due to the differences in the electrotonic distances. However, the difference in the extent of dendritic filtering could not cause such dramatic variations in the shape of EPSCs, since the fluctuations in the shape of pharmacologically isolated NMDA and AMPA EPSC were never so large.

The variations in the kinetics of EPSCs per se may imply that the postsynaptic AMPA and NMDA receptors have the different quantal patterns. For further verification of this hypothesis, the relative NMDA fraction was calculated for each current trace and the PDF of the distribution of the NMDA fraction was calculated for each cell. If the fluctuation of the NMDA and AMPA current occurred synchronously, the PDF would exhibit the rather narrow unimodal distribution with the peak location approximately equal to the ratio of the average NMDA and AMPA components. But this was not the case. In all cells tested the PDF of the relative NMDA fraction exhibited wide peak-like

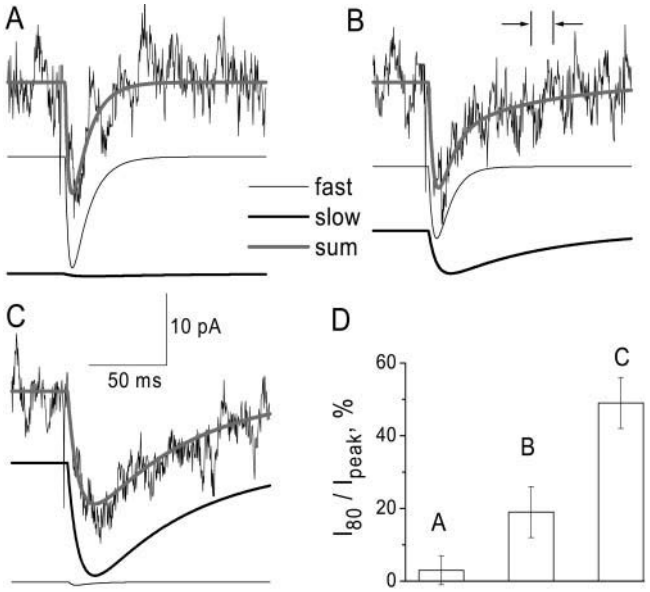

FIGURE 4 Fluctuations in the shape of composite (AMPA and NMDA) EPSC. (*A–C*) Examples of individual composite EPSCs recorded at −50 mV. The traces are fitted with two components, a fast one representing the theoretical AMPA component, and a slow one for the NMDA component. (*D*) The ratio of the amplitude of current measured 80 ms after the peak (as shown in panel *B*: practically mediated only by NMDA receptors) to the peak value. Note the different shape and fractions of the fast and slow components of EPSC, recorded at the same conditions: (*A*) AMPA current, (*B*) composite current, (*C*) NMDA current.

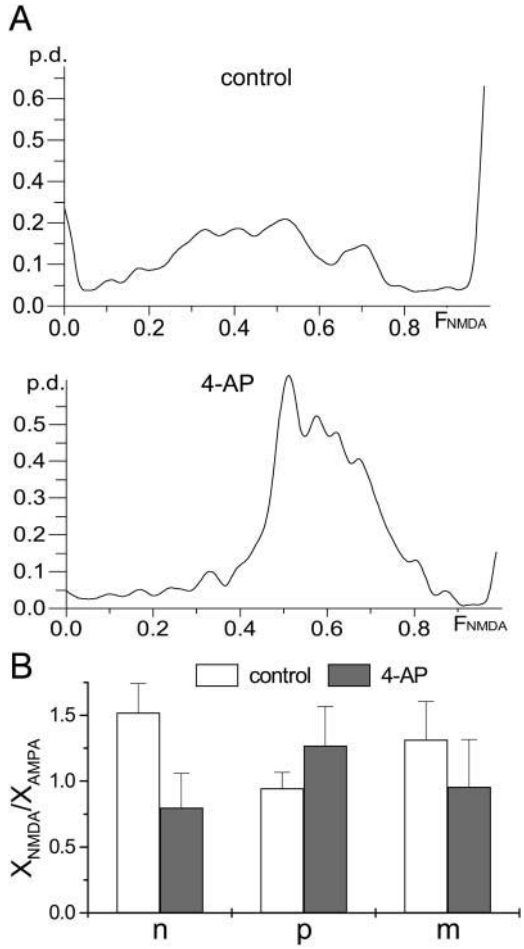

FIGURE 5 The AMPA and NMDA components of composite EPSCs exhibit asynchronous fluctuations. The components were extracted from the composite EPSC on the basis of their kinetics (see Fig. 4). (*A*) An example of PDF for the distribution of the relative fraction of the NMDA component in the composite EPSC recorded in the cell 20/03#4. Note the peaks corresponding to the pure NMDA EPSCs. (*B*) Difference in quantal parameters for AMPA and NMDA components in control conditions and in 4-AP. From left to right, the value X_{NMDA}/X_{AMPA} represents correspondingly the relative ratio of maximal number of quanta, probability of quantal event, and mean number of quanta. Note a significant increase in the maximal number of quanta for AMPA currents under 4-AP.

distribution, accompanied by the narrow peak near the unit value (Fig. 5 *A*). This result suggests the presence of synapses that were ''silent'' with respect to AMPA receptors. Secondly, this result implies that synchronously evoked NMDA and AMPA components of postsynaptic current fluctuate asynchronously.

These conclusions are supported by the generalized data on the changes in quantal parameters (Fig. 5 *B*). In the control conditions, the release probabilities are approximately equal, whereas the maximal number of quanta for the AMPA component is smaller than for NMDA. In 4-AP, the maximal number of quanta for AMPA component increases, whereas the number of quanta for NMDA remains approximately the same. The increase in the release probabilities also was different for AMPA and NMDA components. The changes in the quantal size of AMPA and NMDA components of the EPSC occurred in a similar way to that observed for the pharmacologically isolated currents. The AMPA component did not exhibit significant changes in quantal size, whereas the quantal size of the simultaneously recorded NMDA component increased considerably (by 54 ± 37%).

Taken together, our data suggest different mechanisms of quantization for NMDA and AMPA currents, postsynaptically and presynaptically, respectively, both in control conditions and when transmitter release is enhanced by 4-AP. The most plausible explanation of such difference may be the different levels of saturation of NMDA and AMPA receptors. To further address this issue, the computer simulation was carried out.

Computer simulation of the effects of glutamate spillover and receptor saturation

The time course of activation of AMPA and NMDA receptors after release of different numbers of vesicles was calculated for a wide range of parameters as described in Methods. To take into account the latest data on the asymmetry of glial uptake in the CA1 synapses (Lehre and Rusakov, 2002), the concentration of glutamate transporters was varied in the range of 0.2–2 mM; such a range

corresponds to the postsynaptic density of transporters. The density of extrasynaptic receptors is a very important parameter for estimating the physiological role of glutamate spillover. There is a lack of quantitative morphological data on the density of extrasynaptic glutamate receptors. At the same time, numerous quantitative data suggest that the density of extrasynaptic receptors is very low as compared to the density of receptors inside the synaptic cleft (for review, see Nusser, 2000). That is why we varied the relative density of extrasynaptic receptors in the broad range of 0.001–1.

The results of computer simulation are consistent with our experimental findings. Fig. 6, *A* and *B*, represent NMDA and AMPA synaptic responses simulated for most typical/physiologically relevant parameters; the results of simulation for a broad range of parameters are presented in the Supplementary Material. As one can see from Fig. 6, dependence of the NMDA response on glutamate content exhibits a partial saturation even at high glutamate uptake levels; the 50% activation of postsynaptic NMDA receptors may be reached after release of 1–2 vesicles (3000–6000 molecules). At the same time, the kinetics of the NMDA response in a single synapse becomes slower with increase of glutamate release (data are shown in Fig. S4). The AMPA receptors are much farther from saturation, and the postsynaptic AMPA response grows almost linearly at physiological levels of glutamate release and uptake (Fig. 6 *A*); 50% activation of postsynaptic AMPA receptors is reached after release of 4–6 vesicles.

Such difference in the saturation level may underlie the difference in the quantal behavior. Fig. 6, *C* and *D*, show the

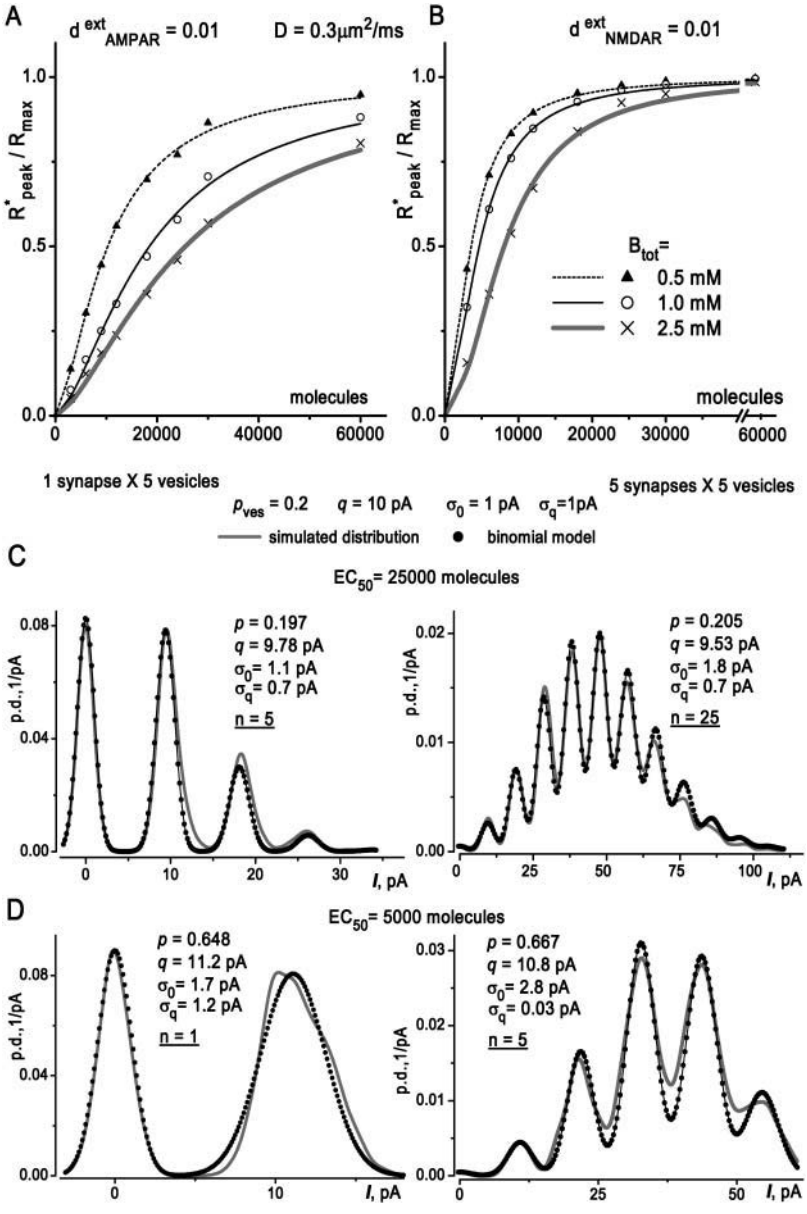

FIGURE 6 Dependence of quantal response on release of glutamate. (*A* and *B*) The computer simulation was made taking into account the spillover of glutamate out of the synaptic cleft, as described in the Methods. The concentration of glutamate transporters B_{tot}, diffusion coefficient D, and relative density of extrasynaptic receptors d^{ext}_{AMPAR} and d^{ext}_{NMDAR} were as indicated. The other parameters of the model were as follows: the effective radius of extrasynaptic space $r_{max} = 500$ nm, spine neck height $z_{max} = 200$ nm, synaptic cleft radius $r_c = 100$ nm, extracellular volume factor $\alpha = 0.12$, tortuosity factor $\lambda = 1.34$. (*A*) The dependence of peak number of open AMPA receptors (R^*_{peak}) on the number of glutamate molecules released. Data were normalized on maximal value (R_{max}) reached at complete saturation of receptors. Lines represent the best fit of data with the Hill equation $R^*/R_{max} = 1/(1+(EC_{50}/G)^n)$, where G is number of glutamate molecules released, EC_{50} is the dose of glutamate producing half-maximal response, and n is Hill's coefficient. The EC_{50} for B_{tot} of 0.5, 1, and 2.5 mM are, respectively: 10,300, 18,700, 25,600; n is in the range of 1.3–1.6. (*B*) Response of postsynaptic NMDA receptors grows sublinearly with release of glutamate. The EC_{50} for B_{tot} of 0.5, 1, and 2.5 mM are, respectively: 3580, 4640, 8030; Hill coefficient is in the range of 1.7–2.1. (*C* and *D*) Impact of the level of receptor saturation on the quantal behavior of the synaptic response. The solid gray lines represent the probability density function for EPSC amplitude distribution simulated using the Monte Carlo procedure as described in Methods. The release of 1 to 5 vesicles containing 3000 molecules each occurred in single (*left panels*) or five (*right* panels) sites with probability $p =$ 0.2. Quantal size q (i.e., average response of each single synapse to a single vesicle) was 10 pA, and the basic (σ_0) and quantal (σ_q) variance were 1 pA; they correspond to the 10% variance in the quantal size and the 10% variance in the vesicle volume. The half-saturation level (EC_{50}) was correspondingly 25,000 (*C*) and 5000 (*D*) molecules. The dotted black lines represent the fit of simulated distributions by the binomial model with incremental quantal variance; probability of quantal event p, quantal size q, basic (σ_0) and quantal (σ_q) variance, and maximal number quanta n were as indicated. Note the good agreement between parameters of parent and fitted distributions when receptors are far from saturation (*C*). At the same time, even partial saturation of response is sufficient to change the quantal pattern (*D*): the number of quanta becomes equal to number of synapses.

amplitude distributions simulated for EC_{50} values typical for AMPA (25,000 molecules) and NMDA (5000 molecules). The distributions were obtained for an almost ideal case: low variance and absence of instrumental noise, so nothing could obscure the quantal peaks of PDF. Nevertheless, the quantal parameters (except quantal size) change dramatically. When the response to a single vesicle is much lower than the level of half saturation (Fig. 6 *C*, *upper graphs*), the maximal number of quanta is equal to the number of vesicles involved (5 and 25, respectively, for 1 and 5 release sites), and quantal probability is close to probability of release of single vesicle. On the contrary, when the response to a single vesicle is close to half (Fig. 6 *D*), the maximal number of quanta becomes equal to the number of release sites (correspondingly, 1 and 5) and quantal probability approaches the probability of nonzero release $p_{>0} = 1 - (1 - p_{\mathrm{ves}})^5 = 0.672$. The above results demonstrate how the partial saturation of receptors may cause the evolution of quantal behavior from presynaptic to postsynaptic quantization.

DISCUSSION

It was previously reported that enhancement of the release of glutamate caused the stimulus-dependent slowdown of the NMDA component of synaptic current at high stimulus strength; this effect was proposed to be due to spillover of glutamate and activation of extrasynaptic receptors (Lozovaya et al., 1999). Nevertheless, there might be some controversy in data interpretation related to the impact of the imperfect voltage clamp on the kinetics and amplitude of the synaptic response measured at soma. In view of the implication of spillover for interpretation of pre- and postsynaptic changes in the synaptic current (Kullmann et al., 1996), we performed a more detailed investigation using minimal stimulation and paying particular attention to any effects of 4-AP on the spatial voltage-clamp conditions. Our novel result not only expands the previous work and strengthens the evidence for spillover, but also demonstrates the striking difference in the impact of spillover and receptor saturation with respect to the two components (AMPA and NMDA) of synaptic transmission. The present paper is aimed primarily at quantal behavior of AMPA and NMDA currents, so special attention has been directed to reliable estimation of their quantal parameters.

Estimation of quantal parameters of EPSC in central synapses

Application of quantal analysis in the central synapses is hampered by the intrinsic heterogeneity of the release probability and quantal size in the population of release sites. The other source of variability arises from the stochastic nature of receptor channel opening (Jonas et al., 1993; Kullmann, 1993). Contributing to the quantal variance, these factors may obscure the quantal distribution of the synaptic current. The existence of quantal amplitude distributions or the possibility of accurate determination of quantal parameters in the central synapses was doubted frequently (Bekkers et al., 1990; Stevens, 1993; Liu and Tsien, 1995). Nevertheless, quantal behavior of the EPSC in hippocampal slices has been repeatedly demonstrated (Liao et al., 1992; Jonas et al., 1993; Stricker et al., 1996; Larkman et al., 1997).

In our experiments, we observed quantal behavior of both AMPA and NMDA components of synaptic transmission in almost all of the CA1 neurons tested. The comparatively high success rate may arise from using the noise-free technique for measuring the EPSC amplitude. We did not intend to investigate the applicability of different models for quantal analysis in hippocampal synapses; we just tried to choose a simple way to discriminate between quantal and nonquantal amplitude distributions and to evaluate quantal parameters. That is why the simplest quantal model—the binomial model—was used. This model uses a small number of parameters. Each of them—size of quanta, probability of quantal event, and maximal number of quanta—is meaningful for the description of synaptic transmission. They can be easily interpreted for both postsynaptic and presynaptic quantization cases. The binomial model is also suitable for analysis of EPSCs originating from several synaptic boutons. Such a situation is very likely for our experimental conditions, since axons of CA3 cells may form multiple contacts with a single CA1 neuron (Sorra and Harris, 1993; Hsia et al., 1998). In view of the intrinsic nonuniformity of quantal parameters, their values calculated by the binomial model for EPSC in slices represent the estimations of average values over the synaptic connections excited.

The reliability of estimation of quantal parameters may be improved due to usage of the maximal likelihood technique in combination with the autocorrelation-based method. The former does not require the finite sampling of the amplitude distribution, and the latter uses no preassumption on distribution law and may be used for independent verification of quantal behavior. The good agreement between data obtained by these methods at different membrane potentials indicates their ability to evaluate the most important parameters, quantal size and mean quantal content, with a fair degree of confidence. Our estimations of release probability, quantal size of AMPA current, and number of receptors involved in a quantal event are in good agreement with the data obtained earlier (Liao et al., 1992; Jonas et al., 1993; Stricker et al., 1996).

Thus, our results demonstrate the feasibility of the simple binomial model for evaluation of the quantal parameters of synaptic currents. Even taking into account the putative inaccuracy of quantal analysis, one can rely on qualitative results which are as follows: change in the quantal size of NMDA current, and lack of change in quantal size and

change of quantal content of AMPA current. Such dramatic differences in quantal behavior may arise from the kinetic properties of AMPA and NMDA receptors.

Impact of receptor saturation on quantal behavior

The saturation of receptors at a single central synapse by a quantum of neurotransmitter is the subject of much controversy. Until recently, it has been widely assumed for hippocampal CA3/CA1 synapses that the content of a single synaptic vesicle is sufficient to saturate both AMPA and NMDA receptors (Tong and Jahr, 1994; Frerking and Wilson, 1996; Bergles et al., 1999). Our data on changes in the quantal size imply a lack of saturation for AMPA receptors and semisaturation for NMDA receptors. These results are in good agreement with recently reported evidence for nonsaturation of AMPA receptors (Liu et al., 1999) and incomplete saturation of NMDA receptors (Mainen et al., 1999) at CA1 synapses. Given the increase in the quantal size in the range of 40–140% (Fig. 3, *C*), one can estimate the level of saturation of the NMDA receptors as 40–70%: this is in good agreement with results of computer simulation. Our data on the partial saturation of glutamate receptors are close to the theoretical estimations of AMPA and NMDA receptor occupancy made by Franks et al. (2002). Also, our results agree closely with the experimental estimate made for dendritic spines of CA1 pyramidal neurons by Mainen et al. (1999). In general outline, the recent data on the saturation of receptors are consistent. The controversy may arise from different interpretations of the term ''saturation,'' since it may be used either in the sense of receptor occupancy by agonist or in the sense of sublinear growth of response with increase in transmitter content (as in the present paper). That is why the EC_{50} value, or number of vesicles causing the half-maximal response, seems to be a more suitable descriptor for analysis of changes in the quantal behavior.

Even partial saturation of postsynaptic receptors has a great influence on quantal behavior and may change the physiological sense of quantal parameters. Theoretically, the impact of saturation may be described by a quantal model with decremental distance between peaks and incremental peak width. However the neighboring peaks can merge because of variability of quantal response. For example, the CV of synaptic response originating from the stochastic opening of 30–80 receptors (at open probability of 0.2–0.5) may reach 0.25. This may be enough to mix up the response to one vesicle and the response to three vesicles if a single vesicle causes 50% occupancy of postsynaptic receptors. When several synapses are activated, the quantal pattern of activity of every single bouton may be obscured more easily because of instrumental noise and variability of quantal size.

Therefore, the complete saturation of receptors is not necessary, and semisaturation also may lead to postsynaptic quantization of synaptic current, as illustrated by Fig. 6. In such a situation the quantal event reflects the activation of the synaptic bouton as a whole rather than the release of a single vesicle. Correspondingly, quantal size represents the response to an average number of vesicles per act of release, maximal number of quanta, and number of release sites; and the quantal probability reflects the probability of nonzero release (release of one or more vesicles) in a single synapse. This is the case when the increase in the amount of released neurotransmitter may cause the increase in the quantal size. It is worthwhile to note that an increase in quantal size would not occur if receptors were saturated completely.

The classical presynaptic quantization may be observed when receptors are far from saturation, so 50% occupancy of the postsynaptic receptors is reached after release of 3–5 vesicles, at least. In this case the quantal probability represents the probability of transmitter release, and maximal quantal number reflects the total number of vesicles ready for the release over all presynaptic sites involved. For the case of presynaptic quantization, the enhancement of transmitter release would hardly result in the increase in quantal size.

Role of glutamate spillover

The level of saturation of intra- and extrasynaptic receptors may be different. When the content of a single vesicle (5000 molecules of glutamate) is released into the synaptic cleft of radius 100 nm and height 20 nm, the estimated concentration of glutamate reaches ~1–10 mM; the same figures are given by physiologically relevant computer simulations (Rusakov and Kullmann, 1998; Lehre and Rusakov, 2002; see also Supplementary Material, Fig. S2). The similar estimate for concentration of glutamate in the vicinity of the dendritic spine gives ~10–100 μM. The apparent EC_{50} of the NMDA receptor estimated based on the commonly accepted kinetic scheme (Lester and Jahr, 1992) is in the range of 1–10 μM; experimental estimation of EC_{50} for a brief pulse of glutamate is 10–100 μM (Chen et al., 2001). Even allowing an order of magnitude of inaccuracy of theoretical estimation of glutamate concentration, one can expect the saturation of intrasynaptic NMDA receptors.

On the contrary, extrasynaptic receptors are far from saturation, and spillover of glutamate outside synaptic cleft (Kullmann et al., 1996; Asztley et al., 1997; Barbour and Hausser, 1997) may lead to involvement of additional NMDA receptors and increase in synaptic current. The contribution of extrasynaptic receptors is much larger after release of several vesicles, and the NMDA-mediated component of synaptic bouton may exhibit a lack of saturation. This hypothesis is in good agreement with the experimental data obtained for single-synaptic boutons by optical methods (Mainen et al., 1999) and our data on the increase in the quantal size of NMDA receptor-mediated EPSC.

What would be the impact of spillover on the AMPA component of synaptic transmission? The kinetics of AMPA receptors differs considerably from the kinetics of NMDA

receptors; AMPA receptors can desensitize rapidly from a single agonist-bound state (Jonas et al., 1993), whereas two agonist molecules are needed for receptor channel opening. The activation of AMPA receptors can prevail over desensitization only at relatively high agonist concentration and EC_{50} value for glutamate amounts up to millimolar range. Hence intrasynaptic AMPA receptors to the synaptic response may be partially saturated, whereas extrasynaptic receptors are very far from saturation. So the AMPA component of the synaptic response should be closer to linear with respect to release of glutamate than the corresponding NMDA component. This conclusion is well illustrated by computer simulations of the net activity of intra- and extrasynaptic receptors (Fig. 6).

In our previous paper (Lozovaya et al., 1999) we demonstrated the impact of spillover on the NMDA component of the synaptic current and suggested the crucial relevance of spillover for the case of enhanced transmitter release in certain pathological states. Our new results here suggest a broader implication of spillover: glutamate spills out of synaptic cleft even with the release of a single vesicle and may activate extrasynaptic NMDA and AMPA receptors as well. Due to the contribution of extrasynaptic receptors, the overall synaptic response gains a more linear and less saturated dependence on release of glutamate.

Changes in the quantal content of NMDA and AMPA currents—role of mono- and multivesicular release

The semisaturation of synaptic receptors is necessary but not a sufficient condition for increase in quantal size. The increase in quantal size also would require the increase in number of vesicles released in the synaptic cleft. Although the issue of release of a single vesicle per single release site is widely accepted for central synapses, the evidence of multivesicular release also has been reported (Tong and Jahr, 1994; Auger and Marty, 2000). The difference in quantal content of NMDA and AMPA currents may help to discriminate between two hypotheses. According to the postsynaptic quantization paradigm, the maximal number of quanta for NMDA current would be equal to the number of release sites involved, whereas this parameter for AMPA current would be the product of the release sites number times the average number of vesicles released in each site. For the case of monovesicular release, there should be no difference in maximal number of quanta.

In control conditions the maximal number of quanta for AMPA current was even less than for NMDA current. Such may be explained by the existence of postsynaptic sites lacking the AMPA receptors (Takumi et al., 1999; Nusser, 2000). Our observation of asynchronous fluctuations of AMPA and NMDA components of EPSC also supports the existence of ''silent AMPA synapses.'' The situation changed to the opposite after application of 4-AP: the maximal number of quanta of AMPA current increased almost twofold while NMDA current exhibited a lack of such changes. Taken together with increase in quantal size of NMDA current, these data suggest the possibility of multivesicular release due to enhancement of calcium influx into presynaptic terminal. Although prolongation of action potential with the aid of 4-AP seems to be a rather artificial way of enhancement of synaptic transmission, the similar mechanisms may cause the potentiation of synaptic current in physiological conditions. This may be possible for many protocols of induction of synaptic plasticity. As demonstrated by Geiger and Jonas (2000), high-frequency stimulation can cause inactivation of K^+-channels and the prolongation of presynaptic action potential. In general, any mechanism of increase in the presynaptic calcium influx might have a similar effect.

CONCLUSIONS

Our main finding was the striking difference in the quantal behavior of NMDA and AMPA synaptic currents under conditions of the enhanced release of neurotransmitter. NMDA current exhibited the increase in quantal size which correlated with slowing down of its kinetics. On the contrary, neither kinetics nor quantal size of AMPA current was altered, whereas the number of quanta considerably increased. These findings not only strengthen our previous evidence of glutamate spillover but also demonstrate the different impact of spillover on the AMPA and NMDA components of synaptic transmission. Moreover, analysis of quantal parameters of EPSCs and results of computer simulation suggest the different mechanisms of quantization of AMPA and NMDA receptor-mediated currents. Such difference arises from different levels of receptor saturation which are governed by intrinsic properties of receptors: the quasi-additive response of nonsaturated AMPA receptors contrasts with the variable involvement of saturated intrasynaptic and nonsaturated extrasynaptic NMDA receptors.

SUPPLEMENTARY MATERIAL

An online supplement to this article can be found by visiting BJ Online at http://www.biophysj.org.

The authors thank Dr. F. A. Edwards, Prof. D. Kullmann, and Prof. R. A. North for early discussion and helpful comments on the manuscript.

This work was supported by The Wellcome Trust and Howard Hughes Medical Institute.

REFERENCES

Asztley, F., G. Erdemli, and D. M. Kullmann. 1997. Extrasynaptic glutamate spillover in the hippocampus: dependence on temperature and the role of active glutamate uptake. *Neuron.* 18:281–293.

Auger, C., and A. Marty. 2000. Quantal currents at single-site synapses. *J. Physiol. (Lond.).* 526:3–11.

Barbour, B., and M. Hausser. 1997. Intersynaptic diffusion of neurotransmitter. *Trends Neurosci.* 20:377–384.

Bekkers, J. M., G. B. Richerson, and C. F. Stevens. 1990. Origin of variability in quantal size in cultured hippocampal neurons and hippocampal slices. *Proc. Natl. Acad. Sci. USA.* 87:5359–5362.

Bergles, A. E., J. S. Diamond, and C. E. Jahr. 1999. Clearance of glutamate inside the synapse and beyond. *Curr. Opin. Neurobiol.* 9:293–298.

Chen, N., J. Ren, L. A. Raymond, and T. H. Murphy. 2001. Changes in agonist concentration dependence that are a function of duration of exposure suggest *N*-methyl-D-aspartate receptor nonsaturation during synaptic stimulation. *Mol. Pharmacol.* 59:212–219.

Franks, K. M., T. M. J. Bartol, and T. J. Sejnowski. 2002. A Monte Carlo model reveals independent signaling at central glutamatergic synapses. *Biophys. J.* 83:2333–2348.

Frerking, M., and M. Wilson. 1996. Saturation of postsynaptic receptors at central synapses? *Curr. Opin. Neurobiol.* 6:395–403.

Geiger, J. R. P., and P. Jonas. 2000. Dynamic control of presynaptic Ca^{2+} inflow by fast-inactivating K^+ channels in hippocampal mossy fiber boutons. *Neuron.* 28:927–939.

Himmelblau, D. M. 1972. Applied Nonlinear Programming. McGraw-Hill, Austin.

Hsia, A. Y., R. C. Malenka, and R. A. Nicoll. 1998. Development of excitatory circuitry in the hippocampus. *J. Neurophysiol.* 79:2013–2024.

Jonas, P., G. Major, and B. Sakmann. 1993. Quantal components of unitary EPSCs at the mossy fibre synapse on CA3 pyramidal cells of rat hippocampus. *J. Physiol. (Lond.).* 472:615–663.

Kullmann, D. M. 1993. Quantal variability of excitatory transmission in the hippocampus: implications for the opening probability of fast glutamate gated cannels. *Proc. Roy. Soc. B.* 253:107–116.

Kullmann, D. M., G. Erdemli, and F. Asztley. 1996. LTP of AMPA and NMDA receptor-mediated signals: evidence for presynaptic expression and extrasynaptic glutamate spillover. *Neuron.* 17:461–474.

Kullmann, D. M., and R. A. Nicoll. 1992. Long-term potentiation is associated with increases in quantal content and quantal amplitude. *Nature.* 357:240–244.

Larkman, A. U., J. J. B. Jack, and K. J. Stratford. 1997. Quantal analysis of excitatory synapses in rat hippocampal CA1 in vitro during low-frequency depression. *J. Physiol. (Lond.).* 505:457–471.

Larkman, A., K. Stratford, and J. J. B. Jack. 1991. Quantal analysis of excitatory action and depression in hippocampal slices. *Nature.* 350:344–347.

Lehre, K. P., and D. A. Rusakov. 2002. Asymmetry of glia near central synapses favors presynaptically directed glutamate escape. *Biophys. J.* 83:125–134.

Lester, R. A., and C. E. Jahr. 1992. NMDA channel behavior depends on agonist affinity. *J. Neurosci.* 12:635–643.

Liao, D., A. Jones, and R. Malinow. 1992. Direct measurement of quantal changes underlying long-term potentiation in CA1 hippocampus. *Neuron.* 9:1089–1097.

Liu, G., S. Choi, and R. W. Tsien. 1999. Variability of neurotransmitter concentration and nonsaturation of postsynaptic AMPA receptors as synapses in hippocampal cultures and slices. *Neuron.* 22:395–409.

Liu, G., and R. W. Tsien. 1995. Properties of synaptic transmission at single hippocampal synaptic boutons. *Nature.* 375:404–408.

Lozovaya, N. A., M. V. Kopanitsa, Y. A. Boychuk, and O. A. Krishtal. 1999. Enhancement of glutamate release uncovers spillover-mediated transmission by N-methyl-D- aspartate receptors in the rat hippocampus. *Neuroscience.* 91:1321–1330.

Mainen, Z. F., R. Malinow, and K. Svoboda. 1999. Synaptic calcium transients in single spines indicate that NMDA receptors are not saturated. *Nature.* 399:151–155.

Major, G., J. Evans, and J. J. B. Jack. 1993. Solutions for transients in arbitrary branching cables: II. Voltage clamp theory. *Biophys. J.* 65:450–468.

Nusser, Z. 2000. AMPA and NMDA receptors: similarities and differences in their synaptic distribution. *Curr. Opin. Neurobiol.* 10:337–341.

Redman, S. 1990. Quantal analysis of synaptic potentials in neurons of the central nervous system. *Physiol. Rev.* 70:165–198.

Rusakov, D. A., and D. M. Kullman. 1998. Extrasynaptic glutamate diffusion in the hippocampus: ultrastructural constraints, uptake, and receptor activation. *J. Neurosci.* 18:3158–3170.

Sorra, K. E., and K. M. Harris. 1993. Occurrence and three-dimensional structure of multiple synapses between individual radiatum axons and their target pyramidal cells in hippocampal area CA1. *J. Neurosci.* 13:3736–3748.

Spruston, N., P. Jonas, and B. Sakmann. 1995. Dendritic glutamate receptor channels in rat hippocampal CA3 and CA1 pyramidal neurons. *J. Physiol. (Lond.).* 482:325–352.

Stratford, K. J., J. J. Jack, and A. U. Larkman. 1997. Calibration of an autocorrelation-based method for determining amplitude histogram reliability and quantal size. *J. Physiol. (Lond).* 505:425–442.

Stevens, C. F. 1993. Quantal release of neurotransmitter and long-term potentiation. *Cell.* 72:55–63.

Stricker, C., A. C. Field, and S. Redman. 1996. Statistical analysis of amplitude fluctuations in EPSCs evoked in rat CA1 pyramidal neurons in vitro. *J. Physiol. (Lond.).* 490:419–441.

Stricker, C., and S. Redman. 1994. Statistical models of synaptic transmission evaluated using the expectation-maximization algorithm. *Biophys. J.* 67:656–670.

Takumi, Y., V. Ramirez-Leon, P. Laake, E. Rivnik, and O. P. Ottersen. 1999. Different modes of expression of AMPA and NMDA receptors in hippocampal synapses. *Nat. Neurosci.* 2:618–624.

Tong, G., and C. E. Jahr. 1994. Multivesicular release from excitatory synapses of cultured hippocampal neurons. *Neuron.* 12:51–59.

Voronin, L. L. 1993. Synaptic Modifications and Memory. Springer-Verlag, Berlin.